

EFFECT OF GEOMETRIC SHAPE ON THE CRUSHING PERFORMANCE OF NATURAL JUTE MAT/EPOXY SPECIMENS UNDER AXIAL QUASI-STATIC COMPRESSION

SABAH SALIM HAMZA^{1*}, MOHD YUHAZRI YAAKOB²,
AL EMRAN BIN ISMAIL³ & SALIH MERI AL ABST⁴

^{1,3}Faculty of Mechanical and Manufacturing Engineering, University Tun Hussein Onn Malaysia (UTHM), Malaysia

¹Al muthana Water Directorate ,General Directorate of Water, Ministry of Municipalities and Public Works, Iraq

²Faculty of Mechanical and Manufacturing Engineering Technology, Universiti Teknikal Malaysia Melaka, Malaysia

⁴Iraqi Cement State Company, Ministry of Industry and Minerals, Baghdad, Iraq

ABSTRACT

The interest in the using of natural composite has been increased significantly in recent years in many engineering fields due to their distinctive characteristics; these as low weights, high-energy dissipation ability, and it's considered eco-friendly. In this paper, an experimental investigation is done on the effect of structure geometry on the crashworthiness characteristics of woven jute mat/epoxy composite specimens. The main objective is to understand the influence of the geometrical shape, and layers numbers on the energy absorption of composite specimens under uniaxial quasi-static loading. The twelve hollow specimens were manufactured by combination of manual lay-up and vacuum bladder moulding technique using bi-directional natural jute mat (with two and three layers) and epoxy resin, each with 50mm inner diameter and 100mm length. Three different cross-sectional shapes were used; the hexagonal, octagonal, and decagonal of specimens. From the current unique experiment, it was exhibited most of the composite samples demonstrated stable and progressive deformation with acceptable repeatability during the test process. It also showed that the deformation characteristics and the energy absorption of the octagonal cross-section shape are better than the other cross-section shapes such as hexagonal and decagonal cross-sections shapes. Furthermore, the three laminated layers contributed to high specific energy absorption (SE) and better crushing efficiency (η_c) for each profile. Overall, the octagonal pattern configuration with three plies can be considered as optimal for crashworthiness of structure application compared to other composite samples.

KEYWORDS: Jute Mat, Geometric Shapes, Axial Compression, Progressive Deformation & Specific Energy Absorption

Received: Jan 23, 2020; **Accepted:** Feb 13, 2020; **Published:** Mar 17, 2020; **Paper Id.:** IJMPERDAPR202058

1. INTRODUCTION

The usage of advanced materials with high strength-to-weight and stiffness-to-weight ratio are highly required mechanical properties for the manufacturing of the structure that is used in the transportation and engineering fields in particular, where reduction of weight is a significant criterion as well as the ability of structural crashworthiness [1-3]. The minimum weight leading to a decrease in fuel consumption and carbon dioxide emissions, thus it contributes to the protection of the environment [1]. However, crashworthiness and occupant protection have become a significant issue in the many fields of engineering, especially in the automobile industry. Crashworthiness characteristic is defined as the ability of the structure to maintain the passengers' compartment in case a collision event[2]. Nowadays, composites are widely used in engineering industries, especially transportation because of

their light weight and obtain good crashworthiness characteristics [4,5]. In general, Composite materials are produced from either synthetic or natural materials. Although Synthetic material has pre-eminent impact performance; however, has disadvantage such as High cost, non-biodegradable, and poor recyclability [3]. Whereas the recent previous studies have been proving that natural fibers are low cost, lightweight, recyclable and biodegradable, which is considered environmentally friendly in addition to their good mechanical and physical characteristics. For that, the Natural reinforced composites are achieving much interest and considered good candidate as an alternative for synthetic materials by manufacturers and researchers [6-9]. Among the various Natural fibers, Jute fibers are the probably most common one due to their novel mechanical characteristics, such as good in tensile strength, elastic modulus, low-density, specific strength, flexible usage, and environmental friendliness [10]. However, in spite of these motivation properties, natural jute is rarely utilized in studying the crashworthiness parameters of composite structures [11]. Therefore, it is necessary to analyze the behaviours of specimen structures experimentally with novel materials under diverse conditions before application action.

Irrespective of the component of structures material, progressive crushing failure and stability during the compression loading are major in determining the higher level of energy absorption [12]. Thus, to achieve the above criteria, there is a consensus that the structural geometry is counting as a key parameter influencing the crashworthiness level of composite material [13, 14]. The report by [15] that the shape and dimension have an effective role in influencing the energy dissipating capability of the composite structure. Palanivelu et al. [16] investigated the effect of geometrical shape on the energy absorption capability of glass/polyester composite specimens. it found that alters in cross-section shape that gives rise to increase energy absorption capacity and better crushing characteristics. Ross et al. [17] studied theoretically and experimentally the buckling pressure of hemi-ellipsoidal domes which made from GRFP. Three aspect ratio of oblate domes were tested under external pressure. It concluded that, when the ratio of dome height/base radius increased from 0.25 to 0.7, the produced buckling pressure increased by (0.420 to 0.900). Ghoushji et al [18] investigated on square natural ramie epoxy composite specimens by utilized three different lengths. it was stated, improvement in crushing behavior and energy absorption are also sensitive to the length of tubes. Many authors [12,19] carried out laboratory works on the crashworthiness characteristics of circular and square cross-section composite tubes. Furthermore, the radial corrugation significantly affects the energy obtain of the composite structures [20].

Other studied, Liu et al. [21] investigated the crushing performance and crashworthiness of non- circular composite tube. a double hat shaped tube made of CFRP. The study concluded that the energy absorption of a double hat shaped tube was slightly higher than the regular tubular shape of composite material, whereas it was twice the value of conventional metal tubes.

On the other hand, Yan et al. [22] studied the influence of internal diameter, length/diameter ratios and layers number of flax fibers/epoxy circular specimens on the crashworthiness parameters. The energy absorption capability is strongly influenced by the geometry of the tube. The number of laminated layers with a considerable length of specimen contributes to the higher energy dissipated capability. Rezaei et al. [23] studied the effect of the size of the inner diameter and the number of layers on the cylindrical E-glass/epoxy composite tubes with the same other parameters. It concluded that the energy absorption capacity increases up to 31.20% with the increase of the inner diameter size for the cylindrical specimen from 40 to 50 mm, as well as when an increase laminate plies up to double times results increment of steady crushing force up to three-time and SE up to 1.39 times. Moreover Ismail et al.[9] searched the crashworthiness characteristic of tubular natural kenaf fibres/epoxy composite specimens. The study pointed out to the possibility of

obtaining higher energy absorption (EA) when using increase layers numbers from two to three plies (increase thickness from 5-7mm)

Large Previous studies [24-28] have demonstrated the fibers orientation along with the axial direction of the tube structure is capable to absorb more energy than other fiber orientations. Therefore, the uni-directional fibre configuration with the above-mentioned factors has been chosen for this work.

In order to avoid catastrophic failure of composite materials due to the transmit loads to the whole profile structure, thus, the trigger mechanism contributes significantly to obtain gradual failure by concentrating the loads on the edge of the profile structure [29]. Reported by Sivagurunathan et al[11], the tulip triggering mechanism can be considered as a favourable design compared to other trigger mechanisms. Therefore, depending on the above-mentioned facts, TT configuration mechanism would be applicable in the current study.

A search of the literature has revealed rarely studies of the effect geometrical shape of natural composite, especially with jute/epoxy materials as energy absorption capabilities. That was the main motivation behind this study. Hence, this search will help to provide more information to the prior contributions to crashworthiness knowledge. Moreover, the effect of laminated layers number on the crashworthiness characteristics of other geometric shapes. All samples were manufactured and tested in the same conditions to ensure a fair comparison among geometric shapes.

2. EXPERIMENTAL PROGRAM

2.1 Specimens' Geometry and Materials

Twelve specimens have been fabricated in the same conditions with three geometrical shapes (octagonal, hexagonal, and decagonal cross-section). Two and three plies of fibers were utilized with bi-direction orientation. The tubes dimensions as shown in tables 1. The specimens fabricated from the jute fibers (in mat form of 1.3 gm/cm³ with bi-directional orientation fibers) is selected as reinforcement. Description of Jute mat/epoxy composite specimens is shown in table 1. The used Epoxy material as matrix, Epoxy resin Auto-Fix (1710-A) and Hardener Auto-Fix (1345-B) are procured by Chemibond company SDN-EHD, Malaysia.

Table 1: Description of Jute Mat/Epoxy Composite Specimen

Type of Specimen	No. of Layers, N	Height H (mm)	Inside Diameter, d (mm)	Number of Specimens
HCS	2, 3	100	50	4
OCS	2, 3	100	50	4
DCS	2,3	100	50	4

2.2 Mandrels Preparation

The second step in the procedure is the preparation of a hollow mandrel. Three geometrical shapes of mandrels were used (hexagonal, octagonal, and decagonal). All mandrels were made by CNC at the workshop from aluminium alloy with 150 mm height, 50 mm outside diameter, curvatures radius of 6 mm around the sharp angles were machined to reduce the stress on profile corners. As depicted in Figure 1.

The mandrels are then wrapped with plastic to prevent the specimens from sticking to the mould, with this process could facilitate the extraction of the specimens from the mould.

2.3 Composite Fabrication

The principle of a combination of manual layup and vacuum bladder technique was employed. For facilitating to the removal of the specimen from the mould, wipe the releasing agent on the surface of the mandrel was applied. The jute mat was trimmed to the proper size of the mould, and then weighed for equivalent epoxy use of the layers. Epoxy and hardener were mixed by an electric mixer at ratio (1:1) as per the supplier's instructions. The electric mixer was used in order to prevent air bubble formation in a mixture. The epoxy resin was poured and spread by using a brush onto the jute layers and then wrapping of the fibers around the mandrel. A steel roller was moved over each jute-epoxy layer under a mild press down to dispose of air bubbles from the laminate and to obtain the required thickness. The peel/release ply, release film, and bleeder film were cut as per the mould size and placed on the surface of layers. The whole specimen was sealed by using a vacuum bag under constant vacuum pressure of 6 bars. Under vacuum, Air bubbles were eliminated and distribution the resin into composite laminate equally. The fabricated specimens were left to cure for 24 h at room temperature ($27c^0 \pm 2\%$). After that, the specimens were extracted from the vacuum bagging and mould. The post-curing was carried out by placing samples into a heat oven at $60 c^0$ for 8 h and $100 c^0$ for 4h. Finally, all tubes were cut into the required specimen size with a height of (100 mm) by using bench saw; a tulip trigger was done by using an angle grinder for each one. This process was repeated four times for each specimen.

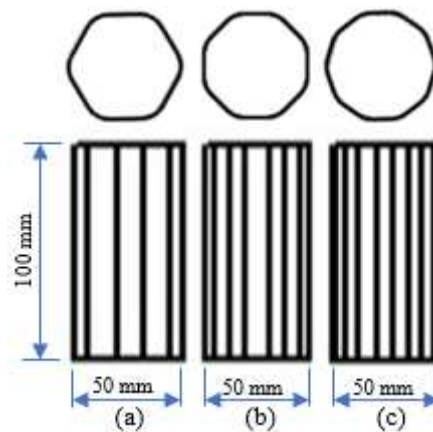


Figure 1: Sketch Diagram for (a) Hexagonal, (b) Octagonal, and (c) Decagonal Specimens.

2.4 Experimental Testing Procedure

All the tests were done under the same conditions for all tubular specimens. Testing of the specimens was performed by applying uniaxial quasi-static compression forces using an Autograph AG-X. In addition, Shimadzu Universal Testing Machine with a 100 kN loading capacity was used, UTEM, Melaka, Malaysia. The testing was conducted based on ASTM: D7336M-16 with stroke set to 80 mm. The crosshead speed was at rate 10 mm/min. Each specimen was positioned on the lower fixed platen and was crushed axially by the parallel platen. Four replicate tests were done for each type of sample with different layers number. Crashworthiness characteristics for each sample can be found from the load-deformation graph under compressive force as depicted in Figure 2.

- Peak load (P_{max}): it is maximum deformation load at the first and second regions with the neglect of the compaction region.
- Mean deformation load (P_m): it is the result of dividing the total energy absorption (EA) in the post-deformation

region to the post-displacement displacement (δ), where, $P_m = (J/mm)$.

- Absorbed deformation energy (AE): it represents the work done of the deformation process, it is calculated as the area underneath the curve of a load-deformation response.
- Specific energy dissipates (SE): it is the ratio of work (AE) done to the crushed mass (m) of the specimen, where, $SE = (J/g)$.
- Deformation load efficiency (η_c): it is calculated from the equation the division of the average load over the greatest deformation load, higher ratio when to be close to unity, where, $\eta_c = \frac{P}{P_f}$.

3. RESULTS AND DISCUSSIONS

The typical force–displacement graph can be distributed into three outstanding regions as in Fig.2. The first region I represents pre-crushing phase, in which the load (P) increases dramatically and reaches an initial maximum load P_{max} within elastic failure behaviour before dropping. In the second region (II), the load fluctuated about a mean load over the crushing process in the plastic failure region and it is associated with the post-crushing phase. The force-displacement graph exhibited the P_{max} , P_m and the displacement of the final failure. In the third region (III), known as the compaction phase, the load increases drastically and non-linearly because of debris accumulations at the end of the tube. This region was not taken into account due to its small absorb energy compare with post-crushing region. The test result was detailed in the next section.

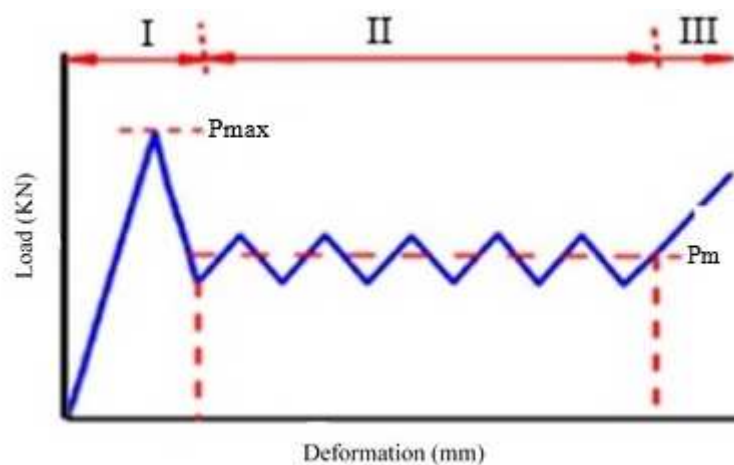


Figure 2: Typical Load vs Deformation Graph.

3.1. LOAD vs Deformation Respons and Failure Mode

3.1.1 Hexagonal Tube (2 Layers)

Figure 3 illustrates the load versus axial deformation history for hexagonal Jute fibres/epoxy composite tube with two layers. It can be observed, at initial phase the load increase non-linearly until reached 4.809 kN at 19.948 mm displacement, which corresponding on the end of triggers. This was due to breakage of material in both inside and outside direction. At pre-crushing phase, the load slightly dropped with plateau level and began steady fluctuated around mean load. This was indicated to start laminate diamond buckling occurred due to lamina bundle folded internal and external

direction (mode II), accompanied with micro-fibres cracks between the folded layers. In the post-crushing phase, the maximum load was 5.064 kN at 27.629 mm. Consequently, the specimen exhibited the progressive diamond folding, which is similar to plastic folding deformation in the thin-wall metal and plastic tube. This mechanism was due to matrix strength higher than interlaminar stress, in addition the fibers have smaller strain to failure compare with matrix. This similar reported by Roslan et al. [30]. Finally, the compaction zone occurred at the last stage when the load reached 2.414 KN due to crushed material densification and has no more material to be crush. However, this zone did not take into consideration because of a little absorb energy compared with the second phase of cycle process. As a result, the main energy absorption, EA was attributed through the progressive plastically deformation of matrix and fibers with no fracturing as well as a few micro-cracks between the folded layers.

3.1.2 Hexagonal Tube (3 Layers)

Figure 4 shows the compression load versus axial deformation history for hexagonal Jute fibres/epoxy composite tube with three layers. It can be observed, at the initial phase the load increase non-linearly until it reached 10.684kN at 23.969mm displacement, which corresponding with the end of the trigger. At pre-crushing zone, the load slightly dropped to 7.538kN and then began fluctuated around the average load but it declined with a plateau level. This was indicated a combination of splaying failure mode and local buckling occurred with starting post-crushing phase. At 57.866mm displacement, the further reduction occurred in load due to the tube's resistance to furthermore buckling. Moreover, intera/interlaminar formation located in this region. The sample attributed the amount of energy absorption (mode II and mode III). The influence of geometry is on the deformation manner of structure. At the last phase, the load increased.

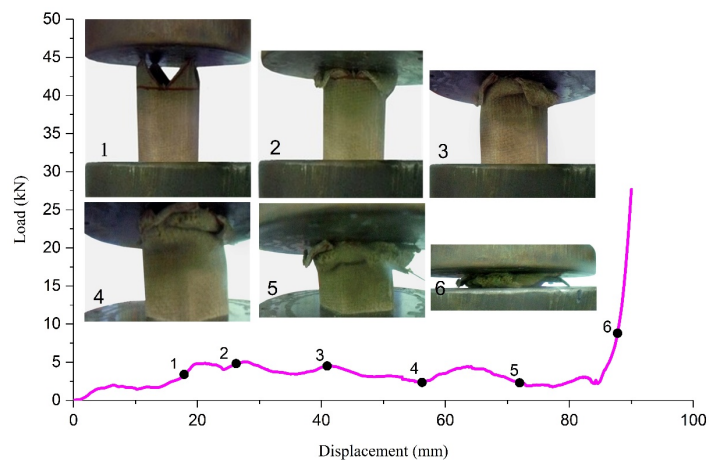


Figure 3: Representative Load vs Displacement and Collapse History of Hexagonal Tube with 2 Layers.

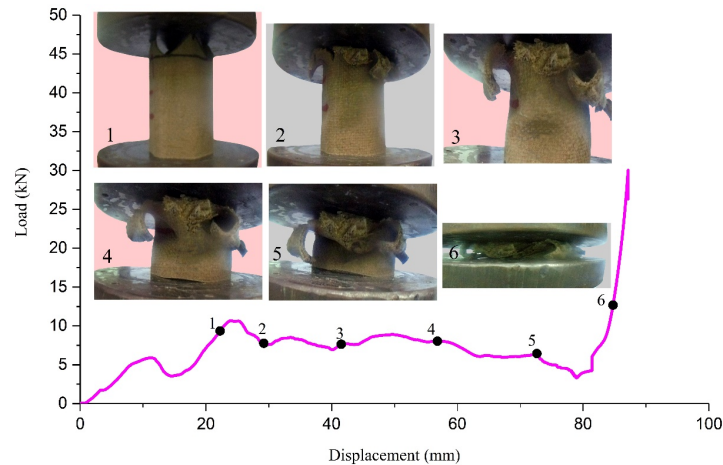


Figure 4: Representative Load vs Displacement and Collapse History of Hexagonal Tube with 3 Layers.

3.1.3 Octagonal Tube (2 Layers)

Figure 5 shows load versus axial deformation history for octagonal Jute fibres/epoxy composite tube with two layers. From above figure, it is observed that once the steel platen contact top of profile the load increase non-linearly until it reached 5.007 kN at 20.71 mm displacement due to breaking the trigger within the pre-crushing phase. The load then dropped slightly and the plateau phase began, fluctuating around the average crushing load as a gradual deformation process. This phenomenon indicated a combination of short lamina bundles bending and transverse shearing mode, which occurred close to the base of tube wall. At the post-crushing phase, the maximum load was 5.359 kN at 25.73 mm displacement. Lamina bundle of specimen subjected to bending, where the laminate fractured at the base of frond that contact with platen press due to natural of brittle material. The brittle fracture manner exhibited stable and progressive failure due to the loads are distributed within the tube. This phenomenon is repeated up to the end of the crushing process. Finally, in the last phase, the loads have dramatically escalated because of the accumulation of all crushed composite materials. However, when a higher load occurs, a somewhat insignificant crushing can be noted. As a result, the pattern attributed a large amount of energy dissipation (Mode II), a combination of a lamina bundle bending and short laminar fracture. In addition, the frictional effect between steel platen moving, adjacent lamina, fronds, and debris wedge. As stated by Palanivelu et al. [16], and [31].

3.1.4 Octagonal Tube (3 Layers)

Figure 6 illustrates the compression versus axial deformation history for Octagonal Jute fibres/epoxy composite tube with three layers. It is observed this specimen test has similar crushing failure mode. However, in the pre-crushing phase with three layers recorded higher peak load than with two layers. The failure began at high initial peak load of 11.504 kN at 26.01 mm displacement. This was referred to the specimen resistant to deformation load. Then the load slightly dropped with plateau level. At the post-crushing phase, the loads fluctuated around average deformation load. This phenomenon clearly indicated to a stable and progressive deformation along this stage due to splaying and short lamina bending with transverse cracking in brittle fracture mode as noted by Yan et al. [22], and Swaminathan et al. [32]. At the last phase, the compaction region occurred when the load reached 8.371 kN, where the load escalated non-linearly and dramatically due to debris densification and crushed materials accumulation. The result, the tube contributed significant energy absorption (mode II) through a combination of lamina bundles bending, transvers shearing, and short axial crack and frictional

effected.

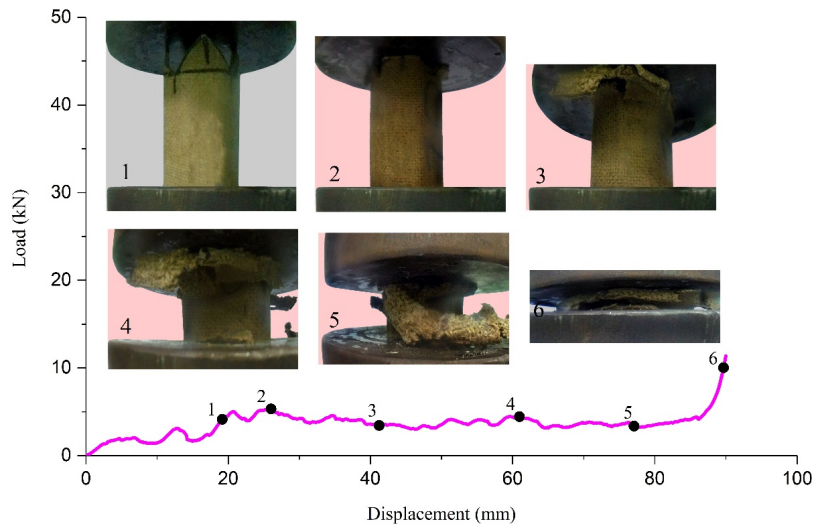


Figure 5: Representative Load vs Displacement and Collapse History of Octagonal Tube with 2 Layers.

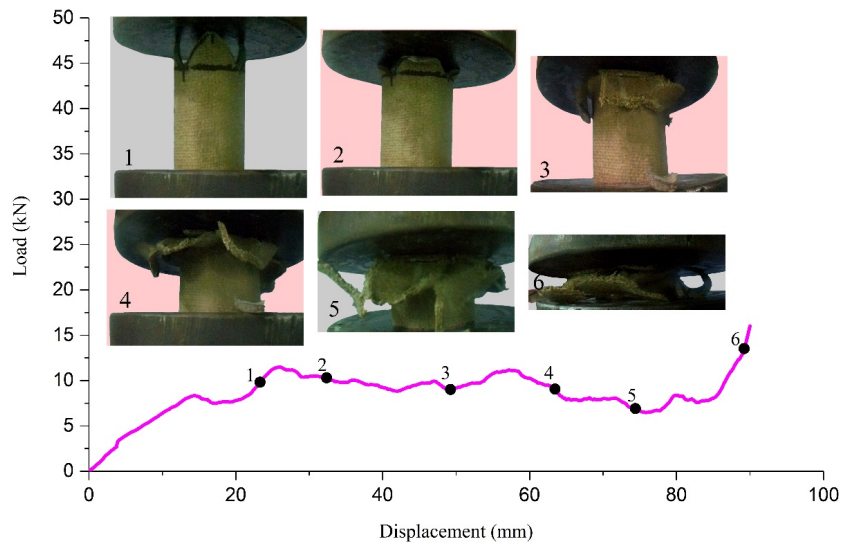


Figure 6: Representative Load vs Displacement and Collapse History of Octagonal Tube with 3 Layers.

3.1.5 Decagonal Tube (2 Layers)

Figure7 illustrates load versus axial crushing history for Octagonal Jute fibres/epoxy composite tube with two layers. From above Fig. ,it is noticed at pre-crushing region, once the steel platen contact profile top the load increase non-linearly until it reached initial peak load of 4.375 kN at 21.343 mm displacement, which is corresponding on crushed triggered end. Then the load dropped slightly and began oscillate around the average crushing load as a gradual deformation process. Fragmentation crushing mode at circumferential of the tube is shown in above top fig. This was due to the formation of shear cracks during the compression process, producing multiple rings of crushed material toward inside and outside of the specimen, which is in the form of short segments. All of these phenomenon’s attribute to geometrical cross-section and

material properties as reported by Bailery et al [33]. At post-crushing zone, the highest load was found 5.601 kN at 30.703 mm displacement. One more at 56.309 mm displacement the sustained load dropped to 2.259 kN due to local buckling occurred at this region before it began to oscillate around the average load, which indicated the specimens' resistance to deformation load. The result, the sample attributed an amount of main energy absorption (Mode II and mode III). Where it less stable than splaying or bending crushing mode, which similar to reported by Greve et al. [34]. Finally, the compaction zone occurred at the last stage when the load reached 4.010 kN due to crushed material densification and has no more material to be crush. The major contribution to the energy absorption was through this failure mechanism, which is the interlaminar cracks growth and fracture of laminate bundles.

3.1.6 Decagonal Tube (3 Layers)

Figure 8 shows load-displacement and crushing history of Decagonal jute fibres/epoxy composite specimens. at the first phase, the load escalated with non-linearly until it reached 9.921 kN at 24.145 mm displacement, which indicated to specimen' s resistance the deformation load. In the pre-crushing, the load dropped sharply until it reached 4.736 kN at 39.228 mm displacement due to buckling at the top and crack longitudinal propagated. Then after the load slightly raised to be sustained fluctuated between 6.001 kN and 7.528 kN within displacement between 43.279 mm and 68.445 mm. this was indicated to brittle fracture failure in post crushing zone occurred. This phenomenon by combine the laminar bundles bending mode and transverse shearing at near of bended frond root. However, from another side observed the buckling started from the top of the profile. This phenomenon due to stress concentrated on the corner of the specimen. Otherwise, after the load reached 68.445 mm displacement further decline occurred because of reduction of load resistance of the remaining specimen part. At the compaction phase, the load increased dramatically due to accumulation and densification of crushed material. The major energy absorption obtained from (mode III) brittle fracture, local buckling, and intera/interlaminar cracks.

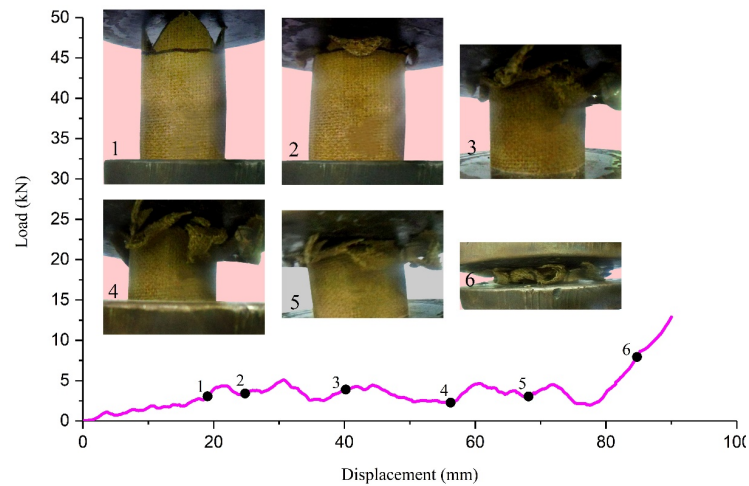


Figure 7: Representative Load vs Displacement and Collapse History of Decagonal Tube with 2 Layers.

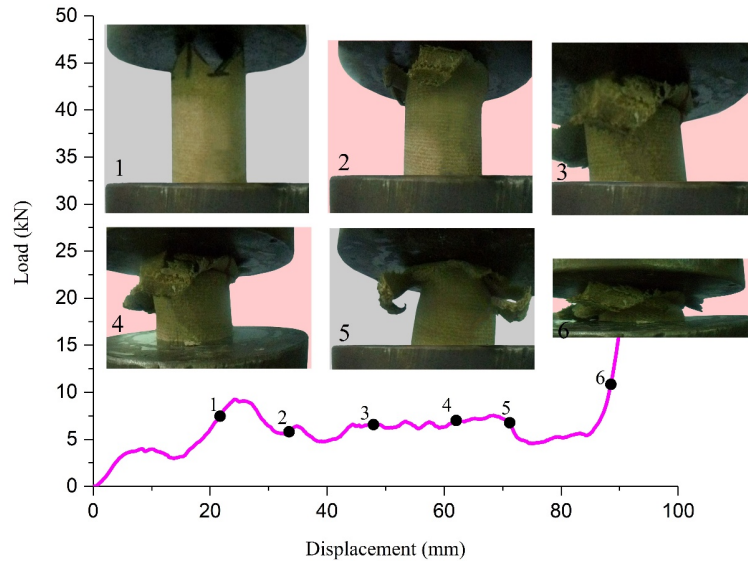


Figure 8: Representative Load vs Displacement and Collapse History of Decagonal Tube with 3 Layers.

4. EVALUATE THE CRASHWORTHINESS PARAMETERS

Table 2 displays the value of crashworthiness parameters. It is obvious; there is the influence of layers number and geometrical shape on crushing performance. To determine the appropriate design, it is necessary to compare and discuss each of the parameters in detail as the following:

Table 2: Average Test of Jut Mat/Epoxy Specimens.

No. of Sa.	No. of Layers	Pmax (kN)	Pm (kN)	Mass (g)	EA (J)	SEA (J)	CFE %
HCS	2	5.30	3.11	22.4	248.74	11.11	58.6
HCS	3	10.68	6.53	32	522.42	16.33	61.1
OCS	2	5.36	3.39	21.6	271.48	12.57	63.3
OCS	3	11.50	8.33	32	666.65	20.83	72.4
DCS	2	5.60	2.97	21.7	237.57	10.95	53.0
DCS	3	9.92	5.63	32.1	450.56	14.04	56.8

4.1. Effect Geometry on Crashworthiness

In general, the most important parameters such as peak load (Pmax), specific energy absorption (SE), and crushing efficiency (η_c) are taken into account to assess the performance of the structure under compression loading test.

4.1.1 Peak Load (Pmax)

Figure 9 shows the peak load values for the different geometric shapes during the loading test which were obtained directly from the load-displacement diagram. It is known as the greatest load that the specimen can withstand before failure occurs during the elastic phase. The high load (hence the high acceleration) of structure, thus lead to a higher probability of permanent deformation of the structure. Therefore it is essential that the Pmax value be minimized as possible while the SE is higher to protect its occupants and interior compartment of a structure during a collision event [35]. In general, Figure 5 shows a correlation between the peak load and the number of laminate layers of the hollow jute mat/epoxy composite specimen. It is obvious, the load on the tube increment noteworthy as the number of layers increase from two to three

layers. This indicated that the thickness of the specimen walls has an effective effect on the level of peak force, which is independent of the cross-section shape. This result similar to reported by Yan et al. [36], and Ghoushji et al. [37]. These raise in p_{max} is quite obviously for the specimen with three laminate layers where the peak load of octagonal, hexagonal, and decagonal cross-section shape is 159.2 kN, 110.1 kN, and 5164.2kN respectively. However, these values of all geometric shapes are considered lower compared to previous studies (e.g jute mat/epoxy with three layers) where Sivagurunathan et al.[11]and[38] stated that the maximum load was 32.58kN and 27.23KN for circle and square respectively. This was because current study used the temperature post-cure cycle for all specimens after fabricated as stated in the recommendations of the supplier company for epoxy. Furthermore, the effect of temperature treatment on the structure is also reported by Xu et al. [39]. In brief, peak load data exhibited comparable values, when an increase in thickness for each kind of tube. Even though each specimen has a different cross-section.

4.1.2 Specific Energy Absorption (SE)

Overall, this is due to the difference in material and weight of each specimen used in studies. The evaluating through total energy absorption to determine the structure's capability to dissipate energy in a stable manner may be misleading [40]. In order to make a more realistic comparison among the geometric specimens, it is based on SE. It represents the efficiency and capability of energy absorbed during deformation of structural, which is defined as the total energy absorption resulting from the sum of the areas trapped between the curve and the horizontal axis of distortion divided by the crushed mass of a specimen [41]. Generally, the higher the magnitude of SE, the effective increase in energy absorption. The major effect and interaction of numbers of specimen's laminator layers on the SE are displayed in Fig.11. It is proved that there is an effect of the thickness of laminar bundles on the value of energy absorbed. The highest value of SE with three layers is compared to double layers, which is independent of cross-section of specimen. As stated by Ude et al.[42]. On the other hand, when considering that the number of layers in the specimens is equal, it is clear that the largest SE value was of the octagonal cross-section shape of 20.83J/g and followed by hexagonal and decagonal with 16.33 J/g and 14.04 J/g respectively. The difference in energy absorption values indicated that the cross-section shape of tubes plays an important role in contributing to an increase or decrease in energy absorption. The similar conclusion was reported by Mathew et al. [14], and Abdewi et al. [15]. In summary, the cross-section shape and number of the laminator layers of the composite tube were proved to be a big effect on the value of energy absorption of structures.

4.1.3 Crush Force Efficiency (η_c)

The mean load plays a major role in determining the shape of the load-deformation diagram, which contributes to the measurement of energy absorption efficiency and stability during a collision process. Crushing efficiency is defined as the main load-to-maximum peak load ratio, which closely correlated to the increase or decrease of acceleration and potential damage to the structure. Therefore, it is desirable and purposely to have a mean load close to the peak load. Ideally, the highest efficiency value is close to unity, which is conducive to the largest area under the curve that is representing stable and progressive energy absorption. Fig.12 clearly depicts the relationship between η_c and the number of specimen's layers, regardless of cross-section configuration. It is noticeable, that the η_c of all specimens increased when the number of laminate plies increased from two to three. The scattering rate was lower than the double layers. Demonstrating greater stability and less accelerated of crushing load. The same conclusion was drawn by Aljibori et al. [43]. On the other hand, if the number of layers is considered the same for all specimens, the shape of the cross-section will play a key role in the crushing efficiency. The highest η_c for 3 layers was 72.4% of the octagonal cross-section, followed by 61.1% and 56.8%

for hexagonal and decagonal cross-section form. Through these data, which gives an indication that the thickness and cross-section form of the Jute mat/epoxy composite specimen are critical parameters in determining and developing the performance of the energy dissipation of the structure during a collision, which corresponds to its findings by Mathew et al. [14] and Palanivelu et al. [16].

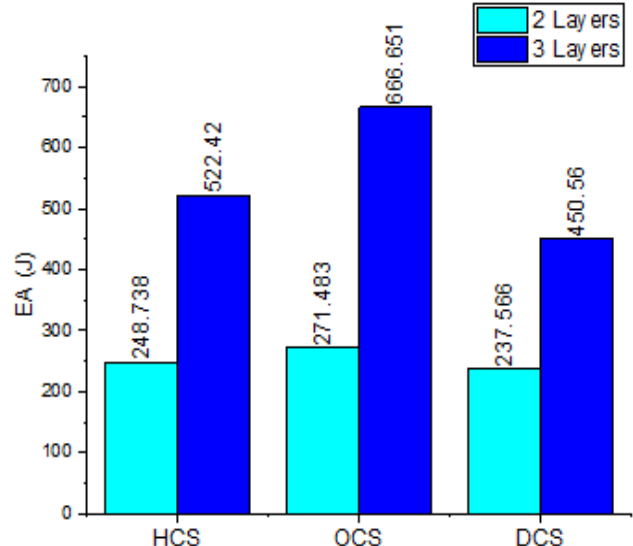
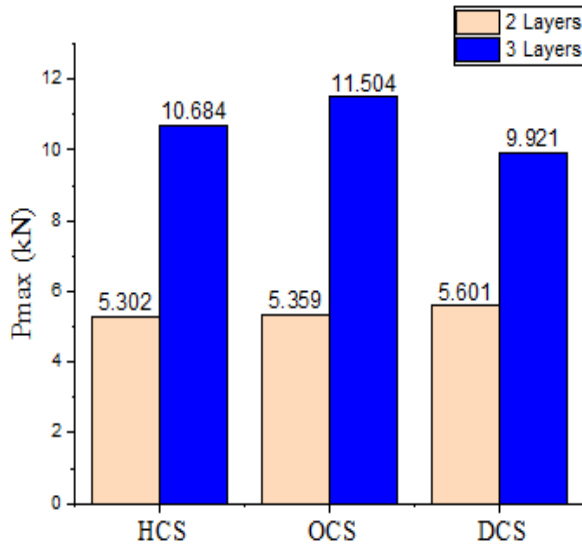


Figure 9: Effect of Geometry on Pmax of the Samples. Figure 10: Effect of Geometry on EA of the Samples.

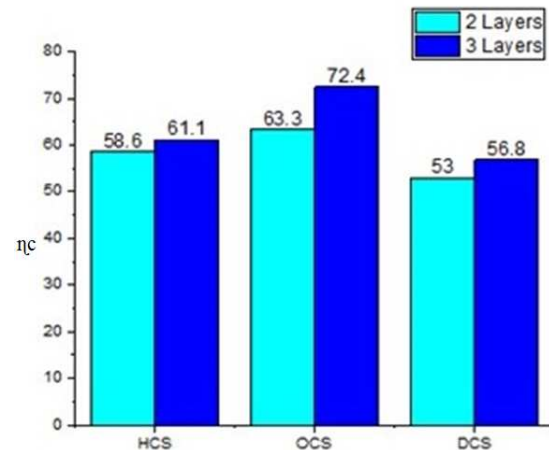
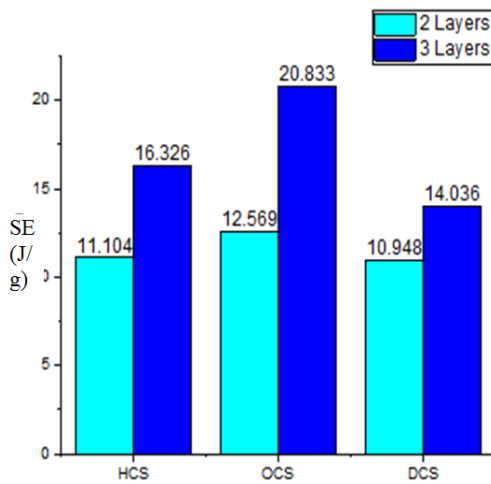


Figure 11: Effect of Geometry on SE of the Samples. Figure 12: Effect of Geometry on ηc of the Samples.

5. COMPARISON

In order to evaluate the performance current work, it is essential to make a comparison with other previous studies using different materials and geometry as shown in table 3.

Table 3: Comparison with Previous Studies

Research	Material	Geometry	Dimension ,mm	SE, J/g
Current study	Jute mat/epoxy	Hexagonal	d=50	16.33
		Octagonal	L=100	20.83
		Decagonal	t=3 layers	14.04

(Balaji et al. 2017),[44]	Aluminium	Square	A=50×50 L=250	8.303
(M.Nalla Mohamed et al. 2017),[45]	Aluminium GFRP/epoxy CFRP/epoxy	Circle	L=150 D= 44 t=3 layers	6.100 7.20 10.28
(Mathew et al.2017),[14]	Silk fabric/epoxy	Different geometry	L=100 t= 1 t/D=0.01- 0.25	51.61- 59.30
(Hussain et al. 2017),[46]	GFRP /epoxy	CylindricalHexagonal Decagonal square	L=120 R= 36 t= 1.829	4.239 4.932 7.345 4.230
(Ghoushji et al. 2016), [37]	Ramie/epoxy	Square	A=80×80 L=50 t=30 layers	16
(Abdewi et al. 2006), [47].	glass fibre/epoxy laminated	Circle corrugated	D=160 L=150 t= 6 layers	10.2 12.2
A.E Ismail 2016), [9].	Kenaf/epoxy	circle	D=70 L=70 t=3 layers	10.98
(Elgalai et al. 2004), [48].	Carbon fibre /epoxy	different corrugation angles	L= 300 D= 100 t=2	13.33- 15.70

As the SE is considered the primary criterion of managing energy reliably in providing the highest degree of safety for the passengers' compartment during the collision. For this, the SE was chosen for fair comparison among other studies. It is observed from Figure 11 that OCS with three layers achieved the highest SE than both HCS and DCS in this work. In addition, it exhibited more stability and less potential to buckle under a quasi-static crushing test due to its failure in brittle mode with a progressive crushing. Furthermore, it achieved the best SE compared to designed structures in different materials and geometry. Thus, it can be considered that Jute mat/epoxy Octagonal specimen outperformed the tubular of (metal, synthetic composite and natural composite) in terms of energy absorption capability.

6. CONCLUSIONS

The 12 specimens were made using jute mat with epoxy. Three different cross-section namely (octagonal hexagonal decagonal) with two different numbers of layers are used in the current study. The objective is to evaluate the crashworthiness characteristics of tubes under compressive quasi-static loading. From the current experiment, it can be seen that different geometric specimens leading to different crashworthiness characteristic with different failure mechanisms too. Based on the results, the conclusion can be summarized as follows:

- Most of jute mat/epoxy composite specimens demonstrated crushing in a brittle mode with a progressive deformation.
- For tubes with a similar cross-section shape, an increase in thickness (number of layers) improve the crashworthiness characteristics values significantly when comparing between three and two layers of each specimen.
- Through this unique study, it has proven that the Structural geometry shape considerably affects the crushing

behavior and the failure mechanism of jute Mat/epoxy composite tubes under quasi-static loading. Thus, the shape of the cross-section contributes to the improvement of the possibility of energy absorption

- The octagonal cross-section tubes with three layers exhibited stable and progressive deformation under axial crushing. The SEA and CFE were 22.4 J/g and 73% respectively, which was higher than HCS and DCS tubes in current work and even it is comparable with previous studies of (metal, synthetic composite, and natural composite).
- V-Compared with previous studies, the usage post - temperature cure for fabricated specimens in this work helped significantly to reduce the peak crush load. e.g. the jute/ epoxy tube which used same number of layers and technic, the peak crushing load was 32.58kN and 27.23KN for circle and square respectively, while the current study shows that the peak crush load from 9- 11kN. Thus, this action contributed to reducing the acceleration that can be transferred to the structure during a collision; thereby obtaining more potential safety measures for occupants inside the compartment.

ACKNOWLEDGEMENT

I thank both of the General Directorate of Water, Ministry of Municipalities and Public Works, Baghdad, Iraq for their financial and moral support in carrying out this research and also to UTHM and Utem Universities for their unremitting efforts to make this work a success.

REFERENCES

1. E. Mahdi, A. S. M. Hamouda, A. S. Mokhtar, and D. L. Majid, "Many aspects to improve damage tolerance of collapsible composite energy absorber devices," *Compos. Struct.*, vol. 67, no. 2 SPEC. ISS., pp. 175–187, 2005.
2. S. E. Stapleton and D. O. Adams, "Crush initiators for increased energy absorption in composite sandwich structures," *J. Sandw. Struct. Mater.*, vol. 10, no. 4, pp. 331–354, 2008.
3. R. A. Eshkoor, S. A. Oshkovr, A. B. Sulong, R. Zulkifli, A. K. Ariffin, and C. H. Azhari, "Comparative research on the crashworthiness characteristics of woven natural silk / epoxy composite tubes," *Mater. Des.*, vol. 47, pp. 248–257, 2013.
4. K. Okubo, T. Fujii, and Y. Yamamoto, "Development of bamboo-based polymer composites and their mechanical properties," *Compos. Part A Appl. Sci. Manuf.*, vol. 35, no. 3, pp. 377–383, 2004.
5. S. T. W. Lau and M. Y. Yaakobc, "Quasi static axial crushing of kenaf fibre reinforced epoxy composite fabricated by vartm method," vol. 12, no. 16, pp. 4804– 4808, 2017.
6. M. F. M. Alkibir, S. M. Sapuan, A. A. Nuraini, and M. R. Ishak, "Effect of geometry on crashworthiness parameters of natural kenaf fibre reinforced composite hexagonal tubes," *J. Mater.*, vol. 60, pp. 85–93, 2014.
7. M. Iqbal, M. Islam, J. Ananda, and K. Lau, "Potentiality of utilising natural textile materials for engineering composites applications," *J. Mater.*, vol. 59, pp. 359–368, 2014.
8. E. Mahdi, A. M. S. Hamouda, and T. A. Sebaey, "The effect of fiber orientation on the energy absorption capability of axially crushed composite tubes," *Mater. Des.*, vol. 56, pp. 923–928, 2014.
9. A. E. Ismail, "Kenaf Fiber Reinforced Composites Tubes as Energy Absorbing Structures," no. 01, pp. 2–6, 2016.
10. A. Kumar and A. Srivastava, "Industrial Engineering & Management Preparation and Mechanical Properties of Jute Fiber Reinforced Epoxy Composites," vol. 6, no. 4, pp. 4–7, 2017.

11. R. Sivagurunathan, S. Lau, and T. Way, "The Effects of Triggering Mechanisms on the Energy Absorption Capability of Circular Jute / Epoxy Composite Tubes under Quasi-Static Axial Loading," 2018.
12. A. Rabiee and H. Ghasemnejad, "Progressive Crushing of Polymer Matrix Composite Tubular Structures : Review," pp. 14–48, 2017.
13. M. F. M. Alkbir, S. M. Sapuan, A. A. Nuraini, and M. R. Ishak, "Fiber properties and crashworthiness parameters of natural fiber-reinforced composite structure: A literature review," *Compos. Struct.*, 2016.
14. A. T. Mathew and A. Thakur, "Experimental study on crushing performance of different geometrical structures woven natural silk epoxy composite tubes," vol. 8, no. 8, pp. 55–66, 2017.
15. E. F. Abdewi, S. Sulaiman, A. M. S. Hamouda, and E. Mahdi, "Quasi-static axial and lateral crushing of radial corrugated composite tubes," *Thin-Walled Struct.*, vol. 46, no. 3, pp. 320–332, 2008.
16. S. Palanivelu et al., "Crushing and energy absorption performance of different geometrical shapes of small-scale glass/polyester composite tubes under quasi-static loading conditions," *Compos. Struct.*, vol. 93, no. 2, pp. 992–1007, 2011.
17. C. T. F. Ross, B. Hock, T. Boon, M. Chong, and M. D. A. Mackney, "The buckling of GRP hemi-ellipsoidal dome shells under external hydrostatic pressure," vol. 30, pp. 691–705, 2003.
18. M. J. Ghoushji, S. Abdullah, R. Zulkifli, A. B. Sulong, and C. H. Azhari, "The failure mode of natural ramie epoxy triggered," no. February, pp. 14–16, 2016.
19. E. Mahdi, A. M. S. Hamouda, B. B. Sahari, and Y. A. Khalid, "On the Collapse of Cotton / Epoxy Tubes under Axial Static Loading," pp. 67–68, 2003.
20. H. S. S. Aljibori, "Energy Systems and Crushing Behavior of Fiber Reinforced Composite Materials," vol. 5, no. 2, pp. 349–355, 2011.
21. Q. Liu, H. Xing, Y. Ju, Z. Ou, and Q. Li, "Quasi-static axial crushing and transverse bending of double hat shaped CFRP tubes," *Compos. Struct.*, vol. 117, pp. 1–11, 2014.
22. L. Yan and N. Chow, "Crashworthiness characteristics of flax fibre reinforced epoxy tubes for energy absorption application," *Mater. Des.*, vol. 51, pp. 629–640, 2013.
23. B. Rezaei, A. Niknejad, H. Assaee, and G. H. Liaghat, "Axial splitting of empty and foam-filled circular composite tubes - An experimental study," *Arch. Civ. Mech. Eng.*, vol. 15, no. 3, pp. 650–662, 2015.
24. Y. Yang, A. Nakai, and H. Hamada, "Effect of collapse trigger mechanism on the energy absorption capability of FRP tubes," *ICCM Int. Conf. Compos. Mater.*, 2007.
25. Huang J, Wang X. On a new crush trigger for energy absorption of composite tubes. *Int J Crashworthiness*. 2010;15:625–34.
26. C. Parameters, H. S. S. Aljibori, K. Firas, M. Alosfur, and N. J. Ridha, "Axial quasi-static crushing behaviour of cylindrical woven kenaf fiber reinforced composites Axial quasi-static crushing behaviour of cylindrical woven kenaf fiber reinforced composites," 2017.
27. L. N. S. Chiu et al., "Crush responses of composite cylinder under quasi-static and dynamic loading," *Compos. Struct.*, vol. 131, pp. 90–98, 2015.
28. A. E. Ismail, "Energy Absorption Performances of Square Winding Kenaf Fiber Reinforced Composite Tubes," vol. 6, no. 6, pp. 2662–2668, 2015.
29. H. Jiang, Y. Ren, B. Gao, J. Xiang, and F. Yuan, "International Journal of Mechanical Sciences Design of novel plug-type

- triggers for composite square tubes : enhancement of energy-absorption capacity and inducing failure mechanisms,” vol. 132, no. June, pp. 113–136, 2017.
30. M. N. Roslan, M. Y. Yahya, Z. Ahmad, and A. R. A. Hani, “Energy absorption behaviour of braided basalt composite tube,” *Adv. Compos. Mater.*, no. November, pp. 1–15, 2017.
 31. S. Palanivelu et al., “Composites : Part B Comparison of the crushing performance of hollow and foam-filled small-scale composite tubes with different geometrical shapes for use in sacrificial cladding structures,” *Compos. Part B*, vol. 41, no. 6, pp. 434–445, 2010.
 32. Rashid, F., K. Dawood, and A. H. M. E. D. Hashim. "Maximizing of solar absorption by (TiO₂-water) nanofluid with glass mixture." *International Journal of Research in Engineering & Technology 2* (2014): 87-90.
 33. N. Swaminathan and R. C. Averill, “Contribution of failure mechanisms to crush energy absorption in a composite tube,” *Mech. Adv. Mater. Struct.*, vol. 13, no. 1, pp. 51–59, 2006.
 34. D. A. Bailey and B. E. Hons, “Engineering and Management The Effect of Damage on the Energy Absorption Potential of Composite Structures,” no. June, 2005.
 35. L. Greve, A. K. Pickett, and F. Payen, “Experimental testing and phenomenological modelling of the fragmentation process of braided carbon / epoxy composite tubes under axial and oblique impact,” vol. 39, pp. 1221–1232, 2008.
 36. R. A. Alia, W. J. Cantwell, G. S. Langdon, S. C. K. Yuen, and G. N. Nurick, “Composites : Part B The energy-absorbing characteristics of composite tube-reinforced foam structures,” *Compos. PART B*, vol. 61, pp. 127–135, 2014.
 37. L. Yan, N. Chouw, and K. Jayaraman, “Effect of triggering and polyurethane foam-filler on axial crushing of natural flax/epoxy composite tubes,” *Mater. Des.*, vol. 56, pp. 528–541, 2014.
 38. M. J. Ghoushji, S. Abdullah, R. Zulkifli, A. B. Sulong, and C. H. Azhari, “Effect of layers stacking number on crashworthiness characteristics of woven natural ramie epoxy,” no. February, pp. 17–18, 2016.
 39. Abou-Rayyan, A. M. "Dynamic Assessment of Cable-Stayed Bridges in Egypt."
 40. R. Sivagurunathan, S. Lau, T. Way, L. Sivagurunathan, and M. Y. Yaakob, “Effects of triggering mechanisms on the crashworthiness characteristics of square woven jute / epoxy composite tubes,” 2018.
 41. J. Xu, Y. Ma, Q. Zhang, T. Sugahara, Y. Yang, and H. Hamada, “Crashworthiness of carbon fiber hybrid composite tubes molded by filament winding,” *Compos. Struct.*, vol. 139, pp. 130–140, 2016.
 42. A. G. Mamalis, D. E. Manolagos, M. B. Ioannidis, and D. P. Papapostolou, “Crashworthy characteristics of axially statically compressed thin-walled square CFRP composite tubes: Experimental,” *Compos. Struct.*, vol. 63, no. 3–4, pp. 347–360, 2004
 43. E. Mahdi and T. A. Sebaey, “Thin-Walled Structures An experimental investigation into crushing behavior of radially stiffened GFRP composite tubes,” *Thin Walled Struct.*, vol. 76, pp. 8–13, 2014.
 44. A. U. Ude, R. A. Eshkoor, and C. H. Azhari, “Crashworthy Characteristics of Axial Quasi-statically Compressed Bombyx mori Composite Cylindrical Tubes : Experimental,” vol. 18, no. 8, pp. 1594–1595, 2017.
 45. H. S. S. Aljibori, “Energy Absorption Characteristics and Crashing Parameters of Filament Glass Fiber / Epoxy Composite Tubes,” no. January 2010, 2014.
 46. G. Balaji and K. Annamalai, “An experimental and numerical scrutiny of crashworthiness variables for square column with V-notch and groove initiators under quasi-static loading,” *Cogent Eng.*, vol. 21, no. May, pp. 1–20, 2017.
 47. M. N. Mohamed and A. P. Kumar, “Numerical and Experimental Study of the Effect of Orientation and Stacking Sequence on

- Petalling of Composite Cylindrical Tubes under Axial Compression,*” *Procedia Eng.*, vol. 173, pp. 1407–1414, 2017.
48. Musalaiah, G., et al. "Experimental Studies on Tensile Properties of Jute Fibre Reinforced Polymer Composites."
49. N. N. Hussain, S. P. Regalla, and V. D. Rao Yendluri, "Numerical investigation into the effect of various trigger configurations on crashworthiness of GFRP crash boxes made of different types of cross sections," *Int. J. Crashworthiness*, vol. 22, no. 5, pp. 565–581, 2017.
50. E. F. Abdewi, S. Sulaiman, A. M. S. Hamouda, and E. Mahdi, "Effect of geometry on the crushing behaviour of laminated corrugated composite tubes," *J. Mater. Process. Technol.*, vol. 172, no. 3, pp. 394–399, 2006.
51. A. M. Elgalai, E. Mahdi, A. M. S. Hamouda, and B. S. Sahari, "Crushing response of composite corrugated tubes to quasi-static axial loading," vol. 66, pp. 665–671, 2004.

